Available online at www.sciencedirect.com
ScienceDirect
Earth and Planetary Science Letters 253 (2007) 513–529
EPSL
www.elsevier.com/locate/epsl

Magma supply, magma ascent and the style of volcanic eruptions

Roberto Scandone [a,*], Katharine V. Cashman [b], Stephen D. Malone [c]

[a] *Dipartimento di Fisica, Università Roma Tre, Via Vasca Navale 84, I-00146, Roma, Italy*
[b] *Department of Geological Science, 1272, University of Oregon, Eugene, OR, 97403–1272, USA*
[c] *Department of Earth and Space Sciences, Box 351310, University of Washington Seattle, WA, 98195, USA*

Received 15 February 2006; received in revised form 27 October 2006; accepted 10 November 2006
Available online 22 December 2006
Editor: C.P. Jaupart

Abstract

We propose a new way of looking at the sequence of events leading to different styles of silicic, volcanic eruptions. Small-to-medium sized eruptions, either explosive or effusive, are explained by the ascent of isolated magma batches from mid-crustal magma chambers. We separate magma ascent into four different zones: the Supply System, the Intermediate Storage System, the Transport System and the Eruptive System. Of primary importance is the concept that ascent from the Intermediate Storage System through the Transport System to the Eruptive System first requires the development of a fracture network. Initially, this fracture network allows the ascent of individual magma batches by opening and then closing after their passage. An increase in the complexity of the fracture network with time increases the connectivity of the fractures and hence the ease of upward magma movement. In this model, the dynamics of the ensuing eruptions are controlled entirely by the time spent in the Transport System. Large explosive eruptions require a full interconnectivity of the Transport System from the Intermediate Storage System to the Eruptive System. Moreover, we suggest that a fully connected conduit is rare, develops only under particular conditions, and typically generates catastrophic eruptions during formation. Here we examine two case histories that illustrate the interplay of these processes: Mt St. Helens, USA, between 1980 and 2004, and Mt. Pinatubo, Philippines, in 1991.

Keywords: Eruption; Mount St. Helens; Pinatubo; Magma ascent; Precursors

1. Introduction

The volumes of individual silicic eruptions range from a few million cubic meters to thousands of cubic kilometers. Resulting eruption styles range from mild lava effusion that lasts days to years, to catastrophic explosions that are over in hours to days; corresponding magma discharge rates are less than one to several million m^3/s. Given this wide range of eruption rate and style, volcanologists can make only qualitative or statistical forecasts of the timing of an impending eruption [1–3]. Moreover, our current understanding of precursory signals does not permit reliable forecasts of eruption size or style. This uncertainty strongly affects decision-making processes related to adoption of prevention measures that may affect the lives of millions of people in densely inhabited volcanic areas, such as those around Vesuvius in Italy, Mt Fuji in Japan or Mt Rainier in the USA. These uncertainties have the potential to impose unnecessary mass-evacuations of urban settlements that could affect the socio-economic state of local communities or even entire regions [4]. For

* Corresponding author. Tel.: +39 0655177250; fax: +39 065579303.
E-mail address: scandone@fis.uniroma3.it (R. Scandone).

0012-821X/$ - see front matter © 2006 Elsevier B.V. All rights reserved.
doi:10.1016/j.epsl.2006.11.016

this reason, a primary goal of modern volcanology is improved understanding of the mechanisms of magma ascent that must precede explosive eruptions, thereby increasing our ability to predict the nature of individual volcanic crises.

1.1. Current models of magmatic systems

Accurate interpretation of geophysical precursors to silicic volcanic eruptions requires models that explain the onset of eruptive activity. It is commonly assumed that overpressure in the magma chamber, arising from crystallization or influx of new magma, eventually opens a conduit to the surface, thus causing an eruption. Subsequent drainage of magma during an eruption releases that overpressure and ultimately terminates the eruption [5,6]. This heuristic model suggests that eruptions should be preceded by a pressure increase within the magma chamber that is sufficiently large to cause upward progressing fracturing of rocks and conduit formation, and that the progress of individual eruptions should be controlled by progressive depressurization. However, predicted pressure changes and magma movement that should be easily detectable by surface deformation and seismic monitoring are rarely seen, while simple depressurization models can be applied only to rare basaltic eruptions.

A more important problem with simple pressure-driven eruption models is the fundamental observation about silicic volcanic eruptions that seismic networks rarely detect obvious upward propagation of volcanic hypocenters suggestive of magma migration [7–9]. Instead, shallow (<6 km) seismic swarms with randomly distributed hypocenters that accompany extensive fracturing of the upper volcanic edifice typically precede eruptive activity by a few hours to months or even years [1,10,11], irrespective of eruption size or style (explosive or effusive). Additionally, eruptions of small- to medium-size commonly comprise a succession of eruptive pulses separated by quiescent periods of weeks to months [12], with each eruptive pulse characterized by its own precursory phenomena, textural character, and water content [13,14]. Together these observations demonstrate that simple views of magma storage and transport systems need to be revised to accommodate not only complex transport models but also detailed observations of the course of individual eruptions.

Critical for interpretation and prediction of volcanic eruptions is a better understanding of the subvolcanic system that stores and transports magma to the surface. Early models of magma storage and transport assumed a mid-to-upper crustal magma chamber that, after the inception of activity, was permanently connected to the surface through a narrow continuous conduit that allowed the passage of either gas-rich magma during explosive eruptions or gas-depleted magma during effusive eruptions [15–17]. According to these models, eruption style was controlled entirely by the nature of the magma within the crustal reservoir, in particular, by the dissolved volatile content.

Work over the past two decades suggests that open-system processes acting during magma ascent may allow both degassing of volatile phases [17,18] and resulting crystallization of anhydrous minerals [19,20], prompting development of a new set of models that examine feedback during magma ascent, degassing, and crystallization [21–23]. These models illustrate the complexity and non-linearity of eruptive behavior that can result from rheological changes arising from phase transitions caused by magma decompression. However, although successful in explaining periodic changes of eruption rate, these models are non-unique and address neither the original formation of volcanic conduits, nor conditions required to end eruptive activity.

1.2. A conceptual model for magma systems

To overcome such difficulties we adopt an alternative approach (see for example Bons et al. 2001, 2004 [24,25]) and hypothesize that small eruptions represent the ascent of individual magma batches detached from the source, as proposed by Gardner et al. [13] to explain the pulsatory character of the Crater Peak eruption in 1992. Furthermore, we suggest that large eruptions occur when the frequency of precursory small magma batches is sufficient to create a fully interconnected magma pathway from the magma storage region to the surface. We explore the implications of this model with regard to the presence or absence of different eruption precursors, inferring how each precursor type might reflect the physical processes that characterize ascent of individual magma batches to the surface. We call the ascending batches “magma quanta” as they represent discrete batches rising from the roots of a volcano under particular material conditions.

To provide a context for the generation and ascent of magma quanta we schematize volcanic systems as four different regions: the Supply system, the Intermediate Storage system, the Transport system and the Eruptive system.

[1] The Supply system refers to everything below the Intermediate Storage system. It includes the feeder complex from the ultimate source of magma in the

mantle as well as temporary storage regions at the mantle–crust boundary or lower crust. We combine this into the Supply System only because the available data are not sufficient to provide detailed constraints on the geometry of this region. In many small eruptions, the Supply System may not participate directly in eruptive activity. Long-lived eruptions, in contrast, may require at least episodic input from the Supply System (e.g. Soufriere Hills, Montserrat [26]). We also discuss the possible role of the Supply System in the cataclysmic eruption of Pinatubo.

[2] The Intermediate Storage system lies at mid- to shallow crustal depths (typically 5–10 km). Here magma arriving from the Supply System may reside for a long time (years to centuries), cooling and differentiating. Magma remains at this level because of (1) a density barrier (neutral buoyancy depth) [27], (2) changes of the stress field, or (3) phase changes within the magma. In many cases, the top of the Intermediate Storage System lies at or slightly above the depth at which the magma becomes saturated in H_2O, a physical condition that will promote both exsolution of a volatile phase and crystallization throughout the magma body [19]. Tapping of the intermediate storage system may be triggered by internal sources (e.g., through a pressure increase because of crystallization), and/or externally (e.g., by influx of new magma, weakening and roof fracture caused by stress corrosion, tectonic stress, or gravitational load). Magma may rise from this region as discrete batches, (as with discrete leaks from a broken container), or, in special cases, as a continuous supply.

[3] The Transport system connects the storage system to the surface and is best imaged using seismic data. Precursory seismicity is typically characterized by swarms of Volcano-Tectonic (VT) earthquakes, indicative of rock fracture. The swarms occur in the upper part of the volcanic edifice (normally from the surface to 4–6 km) without any clear upward migration and usually fade out after the beginning of the eruption [7,8,28]. Initial fracturing may be caused by either external triggering (variation of the regional stress field) or by failure of the internal structure of the volcano, perhaps by interaction of volatiles and heat from the magma storage system. Once a fracture network has been created, buoyant magma can enter the system. When the ascent rate prevails over the supply rate, magma will ascend as an individual magma batch (quantum). Individual fracture pathways may be used repeatedly or alternative pathways may develop. At any one time, the proportion of magma-filled cracks is controlled by the ratio between the injection flux from the storage system and crack velocity [29]. After injection, the ascent velocity of a magma-filled crack is controlled by (1) a buoyancy force arising from the difference between the density of the liquid and that of the surrounding rocks, (2) the viscosity of the magma [29–31] and (3) the stress field along the pathway. Ascent may occur in a stepwise fashion if discontinuities along the path control the size and velocity of ascending quanta [24,25] or if syn-eruptive degassing and crystallization are sufficient to cause temporary magma arrest [21–23]. From this perspective, volcanic eruptions are controlled primarily by the balance between magma buoyancy and the local stress field.

[4] The Eruptive system is the shallow region from which magma is erupted. An eruption is effusive if the magma loses most of its volatiles during ascent through the transport system, otherwise it is explosive. In the latter case, the eruption ends when most or all of a given magma batch is fragmented by the explosive action of volatiles. The loss of gas is strongly controlled by the time spent in the upper part of the Transport System. If the time is short, large super-saturations are required for the nucleation and growth of bubbles [33] and vesiculation proceeds rapidly to magmatic fragmentation. Longer times permit both efficient pre-eruptive degassing by either two-phase flow or gas loss through a permeable network [17,18] and microlite growth [19,20] in response to that degassing, both of which promote effusive rather than explosive activity.

In this paper we focus primarily on the development and evolution of the transport system. Before examining specific case histories, we feel it important to make a few more points about its development. First, it appears that fracturing of the transport system may precede (by days to months) introduction of magma into the fractures [7,8]. Second, several authors have suggested that magma rises to the surface either by opening the upper crack tip and closing the lower one [30] or by developing a bulbous head connected to the source by a thin tail and propagating with constant velocity (stationary regime) [29,31]. Instead, we regard the ascent of magma quanta as the passive response of the Intermediate Storage to the mechanical failure of the Transport System, with each magma quantum a transient pressure wave. The preformed fracture network with deformable walls first opens in response to increased pressure and then closes upon passage of the quantum, a closure mechanism that is different from that proposed by Weertman [30].

What is the role of volatiles in this process? Exsolution of volatiles to form bubbles will increase both magma buoyancy, by decreasing its density, and viscosity, by removal of volatiles from the melt. Recent experiments show that homogeneous bubble nucleation in silicic magmas requires very large supersaturations ($\Delta P \sim 150$ MPa) regardless of decompression rate [32] (Fig. 1a). Moreover, preserved vesicle textures in silicic pumice (even those with abundant phenocrysts) appear to require homogeneous bubble nucleation, at least during rapid magma ascent that accompanies explosive activity [33,34]. Thus it is possible that low-viscosity, volatile-rich magmas may rise to high levels in the volcanic system before extensive vesiculation occurs. By analogy, we suggest that slow initial magma rise may also generate large bubble nucleation delays, allowing magma to ascend aseismically to ~ 50 MPa (Fig. 1a). At this point, experimental data [32] show that bubble growth may be accompanied by extensive gas escape (Fig. 1b), consistent with observed confinement of Long Period (LP) earthquakes and tremor, usually interpreted as signs of gas escape, to very shallow levels (<2 km).

As a final point, we reiterate that the four regions that we have identified as important to transport of magma from the lower crust to the Earth′s surface are not necessarily simultaneously connected. When the magma supply rate is sufficiently low, detachment of magma batches from the Intermediate Storage System inhibits development of a continuous magma-filled conduit to the surface and eruptions, if they occur at all, are pulsatory and of fairly small volume. Only in special cases are the Intermediate Storage System and the Eruption System fully interconnected. When this happens, the most common result is rapid and continuous flow of large amounts of magma that drains the Storage System, often causing caldera collapse. However, there are examples of persistent, dominantly effusive, activity that may also require semi-permanent conduits between the crustal magma chamber and the surface.

Below we apply this conceptual model to two well-studied eruptions, those of Mount St. Helens, USA, 1980–1986 and Mt. Pinatubo, Philippines, 1991–1992. In particular, we relate eruptive precursors to development of the Transport System, explain the onset of the eruption climax, and interpret subsequent patterns of eruptive activity accompanying the waning of eruption intensity in the months to years following the climactic event. Our primary goal is to examine the evolution of the storage, transport and eruptive systems, particularly for cases where we believe that a simple connected–conduit model does not explain the full course of eruptive activity.

2. Discrete–continuous–discrete eruption transitions of Mount St. Helens between 1980 and 1986

2.1. Observations

Mount St. Helens awoke with the onset of significant shallow seismic activity on March 20, 1980. The first eruptions began on March 27, 1980, as a series of

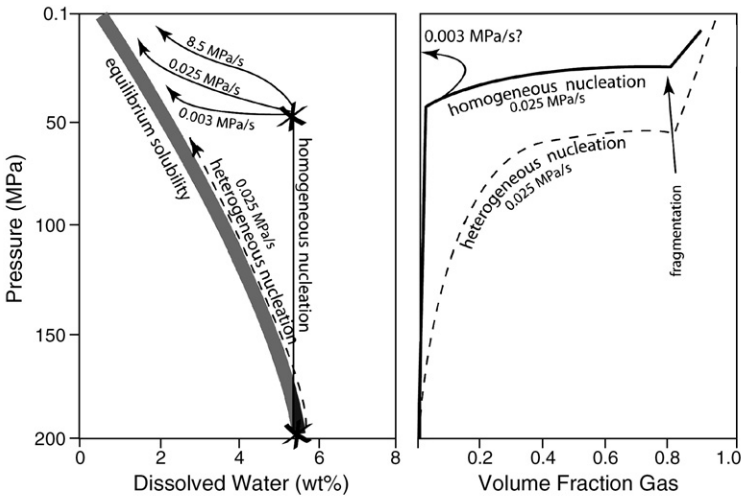

Fig. 1. (a) Variations in dissolved water content as a function of pressure for conditions of heterogeneous (equilibrium) and homogeneous (delayed) bubble nucleation. Asterisks represent pressure of initial bubble nucleation; curves at shallow pressure are labeled for different rates of decompression (Figure modified from [32]). (b) Variations in volume fraction gas for the same conditions as illustrated in (a). Homogeneous and heterogeneous bubble nucleation paths at ascent rates of 0.025 MPa/s are based on numerical simulations for flow through a uniform conduit [35]; hypothetical curve for the slower decompression rate is based on experimental evidence for efficient bubble coalescence and volatile loss under these conditions [32].

intermittent phreato-magmatic explosions [35,36]. Precursory activity culminated in a medium-sized (VEI 5) climactic eruption on May 18, 1980. Subsequent activity was characterized by episodic eruptions with declining explosivity through October 1980, and by predominantly effusive, episodic eruptions through October 1986. A long quiescence then preceded a new period of continuous effusive activity that commenced in the fall of 2004.

The development of the transport system at Mount St. Helens during the weeks prior to the climactic eruption was marked, most notably, by intrusion of 0.11 km^3 of magma into the volcanic edifice to form a cryptodome. Analysis of seismicity between late March and May 18, 1980, shows that magma first arrived at shallow depths as early as March 27, one week after the onset of VT seismicity. If initiation of magma ascent from the Intermediate Storage System (8 km) coincides with beginning of the unrest (20 March), the ascent rate was ~ 0.01 m/s. Episodic tremor [10] after the 31st of March accompanied individual intrusion episodes, which also produced phreatomagmatic explosions [36]. LP earthquakes commenced at the beginning of April, signaling degassing of magma that was accumulating at shallow depths within the edifice. This degassed and growing crypto-dome caused massive deformation of the volcano′s north flank [37] and produced seismicity that was confined to the shallowest part of the edifice.

A break in phreatomagmatic activity occurred between April 22 and May 8, 1980. This hiatus was characterized by a lack of tremor episodes and an abrupt decrease in the seismic energy release of Long Period (LP) earthquakes, suggesting an absence of intrusions during this time period. Renewal of phreatomagmatic explosions on May 8 accompanied new tremor episodes [10], an increase in the seismic energy release of LP earthquakes, and an increase in deformation rate [37]. To summarize, the association of tremor episodes, LP earthquakes, and edifice deformation with phreatomagmatic explosions suggests that the cryptodome was being fed by episodic arrival of magma rather than by steady magma supply through a well established conduit. These features are illustrated in Fig. 2, which shows the sporadic nature of precursory tremor (Fig. 2A), the changing rates of seismic energy release (Fig. 2B), and non-steady edifice deformation during the weeks preceding the climactic eruption (Fig. 2C,D).

The intrusion of magma eventually provoked a catastrophic failure of the volcano′s north flank, which created a massive landslide and concurrent lateral blast at 08:32 PDT on May 18, 1980. The lateral blast lasted for 15 min [38] and produced pyroclastic density currents that devastated an area of approximately 600 km^2 and a co-ignimbrite column that reached a height of 30–32 km. The blast was followed by a period of minor explosive activity followed by the formation of a vertical eruption column from the newly created crater. A US Forest Service radio log [39] notes that eruption intensity increased from 9:25 to 10:36, then decreased from 11:15 to 12:17, then increased again with the onset of the main phase of the eruption. A change in the color and character of the eruption column marked the start of pyroclastic flow activity at 12:17, which lasted for about 4 h [39,40] as magma discharge rate steadily increased. Eruption intensity peaked at 16:30, after which time a sustained vertical column was re-established and the eruption intensity progressively waned until the eruption ended between 18:00 and 18:30.

Eruptions during the summer of 1980 were characterized by discrete, predominantly explosive pulses, that diminished in both volume and duration through time [38]. Each eruption was preceded by limited seismicity and local deformation; the limited duration of precursory activity suggests ascent velocities of 0.1 to 0.7 m/s for individual batches. Explosive eruptions in June, August and October were followed by emplacement of a lava dome in the central crater at average magma ascent velocities ~ 0.01 m/s. The textural characteristics of the erupted magma point to rapid ascent of individual magma batches through the transport system with consequent limited syn-eruptive degassing, although rising magma batches clearly incorporated magma that was residing at shallower levels within the transport system between eruptive events [41,42]. Although measured SO_2 emissions during explosive eruptions of this period are well explained by measured S in the melt [41], extensive degassing of SO_2 and CO_2 measured during inter-eruptive periods [43] led to total volatile emissions exceeding the amount of SO_2 dissolved within the volume of erupted magma.

Between May and December 1980, deformation data showed a gradual subsidence of the volcanic edifice [44], reflecting the readjustment of the volcano following the removal of the magma erupted on May 18 from the intermediate storage system [38]. This subsidence was followed by slight but regular increase in background seismicity between 1980 and 1983 [45] that indicates a slow increase of stress in the highly fractured subsurface. Additionally, the increased duration of eruption precursors from a few hours in the summer of 1980 to a few days or weeks in the following years, suggests a gradual decrease in the average rate of magma ascent. The depth distribution of seismicity during this time period indicates the development of a

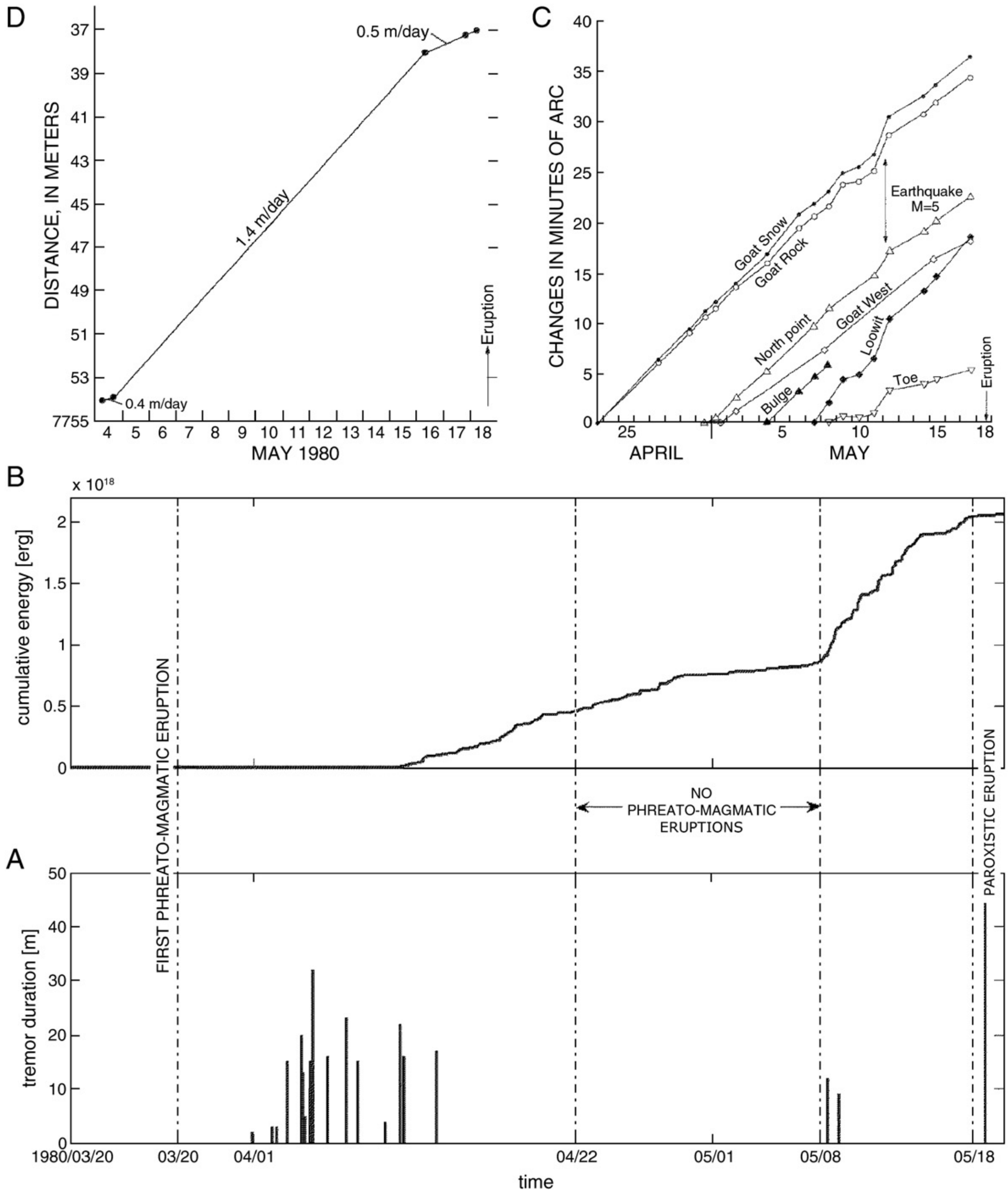

Fig. 2. Temporal variation of geophysical precursors between March 20 and May, 18, 1980 at Mount St. Helens. A) Duration of tremor episodes. B) Cumulative energy release of LP earthquakes as measured at SHW seismic station. C) Changes in horizontal angle, measured by theodolite from Timberline and Toutle [37]. D) Changes in slope distances measured by Geodimeter between Coldwater 2 and Goat Saddle [37]). The observed change in the deformation rates occurs in coincidence with the large increase in LP energy release after May 8.

barrier located at a depth of 2–3 km below the volcanic edifice (Fig. 3). Temporary storage of magma below this barrier is also suggested by the low H_2O contents (shallow equilibration pressures) of plagioclase-hosted melt inclusions and the appearance of a plagioclase microphenocryst population in the dome lavas [41,46,47]. Precursors to each effusive pulse started days to a few weeks before the eruption and included

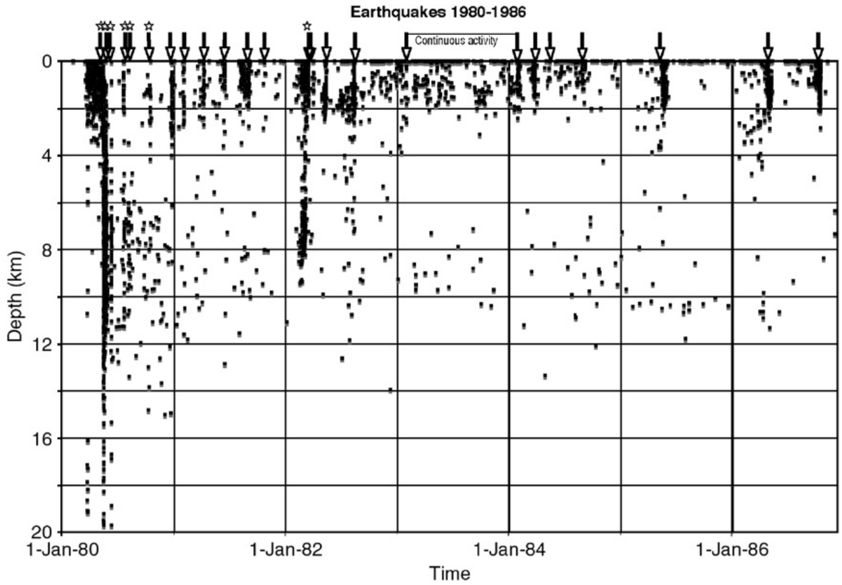

Fig. 3. Time–depth distribution of the seismicity at Mt St. Helens in the period between 1980 and 1986. The precursory activity before each eruption is confined to the top 2–3 km, deeper seismicity occurs after the major explosive eruptions and just before the 1982 mildly explosive eruption. The arrows indicate eruptions, the stars the explosive ones.

shallow (<2–3 km) LP earthquakes and deformation of the dome and surrounding crater floor. The DRE volume of magma produced in individual eruptive episodes between July 1980 and February 1983 remained approximately constant at $2–4 \times 10^6$ m^3 [38,48].

The eruptive system then changed dramatically in February 1983 with the onset of steady effusion. A year of continuous activity produced $>20 \times 10^6$ m^3 of lava, at an average rate of 0.6 m^3/s. A year-long swarm of shallow LP earthquakes accompanied the effusion.

Renewed exogenous dome-building episodes characterized eruptive activity from March 1984 until October 1986. Although the erupted volumes of these late episodes were generally larger than those of episodes before 1983, the inter-eruptive intervals were also longer, leading to an overall decrease in the time-averaged magma eruption rate [48]. At the same time the character of individual eruptions changed, involving an increasing component of endogenous dome growth [49]. Precursory seismicity also changed, with (1) the occurrence of shallow medium frequency earthquakes and (2) the appearance of earthquakes with nearly identical waveforms (multiplets) [50]. Collectively, these characteristics suggest an increasing brittle response of the shallow crust to the intrusion of magma with an accompanying increase in the probability of magma arrest within the transport system. Interestingly, these magma batches were also measurably cooler than earlier batches [49,46], another sign of slower magma ascent.

After cessation of activity in 1986, episodic seismic swarms of VT earthquakes occurred at depths of 2–10 km, indicating continued magma intrusion beneath the seismic lid, although the absence of eruptions during this time period demonstrates that magma failed to penetrate the barrier (Fig. 4). A gradual increase in barrier depth with time suggests it to be at least partially thermal in nature. Seismic data show that intrusions were accompanied by brittle fracturing of rocks within a compressive stress field in the lower part of the transport system, as reflected in earthquake focal mechanism studies [50–52]. Renewed volcanic activity initiated in September 2004, with new magma first appearing at the surface in October 2004. Since that time, lava effusion has been slow and steady (~1–2 m^3/s) and has been accompanied by seismicity only above the shallow barrier, suggesting remobilization of magma intruded during the inter-eruptive period. However, the lack of significant edifice deformation indicates that at least some of this shallow magma is being replenished through the Transport System, perhaps in very small but frequent batches. Evaluations made by Iwatsubo et al. [53] using a Mogi model in an elastic half-space suggest that displacements measured by the geodetic network outside the crater could detect only volumes larger than 2.5×10^6 m^3 at a depth of about 1 km below the crater. The same authors state that the external network was unable to detect any deformation caused by the eruption of 77×10^6 m^3 of lava in the period between 1980 and 1986.

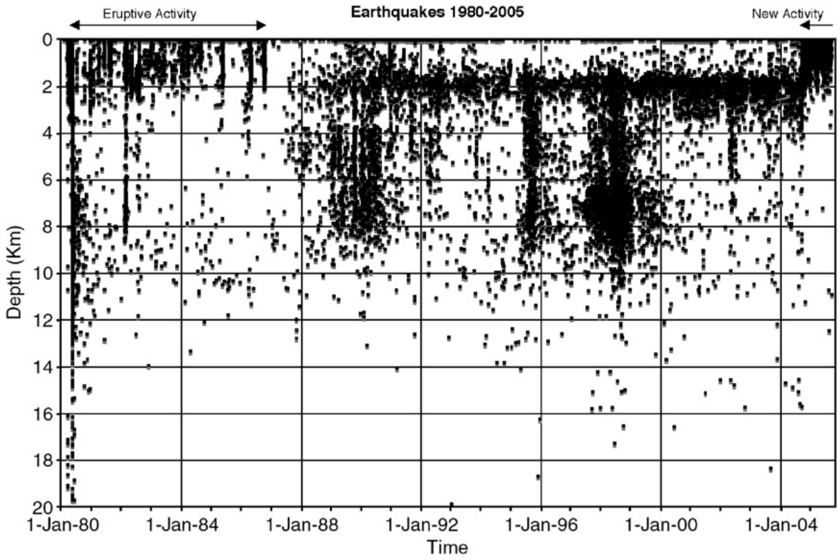

Fig. 4. Time–depth distribution of the seismicity at Mt St. Helens in the period between 1980 and 2005. After 1986, seismicity is mostly confined to depth around 2–3 km, indicating a cap or barrier to upward magma migration and periodic bursts of small events around the Intermediate Storage and the Transport system, indicating several intrusion episodes before the renewal of the eruptive activity in 2004.

2.2. Interpretation

We suggest that the complex eruptive history of Mount St. Helens described above can be explained by periodic–episodic ascent of magma quanta from the Intermediate Storage system. Moreover, we show that this conceptual model explains more of the observational data than models where eruptions are modulated by rheologic changes within shallow levels of the magma conduit. These observations include the episodic nature of precursory activity, the time lag between the edifice failure and the climax of the May 18 eruption, the gradual change from explosive to effusive activity, the near-constant volume of the effusive eruptions, and the seismic swarms that followed cessation of eruptive activity in 1986.

Precursory activity at Mount St. Helens was episodic, as illustrated by seismic and deformation data as well as monitoring of precursory explosion frequency (Fig. 2). This non-steady precursory pattern appears best explained by episodic injection of magma batches (quanta) into the volcanic edifice. It appears that individual quanta were small enough to pass undetected by the external geodetic monitoring network and were practically aseismic, but for tremor episodes, until they reached the volcanic edifice. The lack of deep and intermediate VT seismicity during this time period may reflect delay of vesiculation (and thus accompanying water exsolution from the melt) until shallow levels (Fig. 1) or non-brittle behavior of the hotter lower crust. Extensive shallow degassing is demonstrated by the low H_2O content of plagioclase melt inclusions in cryptodome samples [20] as well as by the shallow distribution of LP earthquakes that accompanied the tremor episodes. Moreover, high supersaturations created by sudden and extensive shallow degassing may explain the extraordinarily high crystal number density of cryptodome samples [34,36].

The May 18 eruption sequence was triggered by catastrophic failure of the north flank of the volcano about one week after an intrusion episode signaled by two tremor episodes and an increase in the deformation rate. Following the lateral blast, sudden removal of the mountain′s top would have created a downward-propagating decompression wave. The volume of magma affected by this initial decompression can be estimated by integrating the eruption rates of Harris et al. [54] for the time period between 9:00 and 12:17 (the onset of climactic activity) and assuming that the volume of pyroclastic flows during this phase was small. This estimate gives a value of about 28×10^6 m^3 of magma, which is equivalent to a cylinder of dense magma of 50 m radius [39,55] extending to 3.3 km, much shorter than the conduit hypothesized to feed the plinian phase [55]. We interpret these data to mean that decompression caused vesiculation and fragmentation of successive magma quanta already migrating upward along the transport system. Intersection of separate magma batches would also explain the fluctuations observed in explosive activity for the subsequent 3 h.

Full interconnection between the intermediate storage system and the eruption system probably occurred after 12:17, when a sudden increase in eruption rate produced massive pyroclastic flows. The 3:45 h time-lag between the landslide and the main phase of the eruption is thus interpreted to reflect the time required for the arrival of magma rising from a depth of about 6–12 km [20,38,39] through a fully interconnected conduit. A time-lag of 3.5 h suggests an average ascent velocity of 0.4–0.9 m/s. Starting in the afternoon of May 18, VT earthquakes increased in size, number, and depth, indicating that the Transport system and upper parts of the Intermediate Storage system were undergoing extensive fracturing due to the rapid withdrawal of magma [38,56]. Collapse of the transport system ultimately terminated the eruption. That eruption termination was not the consequence of diminishing magma supply is indicated by the considerable volume of magma left in the Storage system, magma that generated a large explosive eruption a week later, on May 25.

Activity following the climactic eruption marked a return to episodic ascent of magma quanta. Both rapid ascent (short precursory period) of magma quanta and weak precursory signals reflect the ease of magma rise through the extensively fractured transport system. High inter-eruptive gas fluxes suggest direct degassing from the Intermediate Storage system through an interconnected fracture network [41,43,57], providing evidence for an open fracture network during this time period. An open and moderately well connected system is also suggested by the pyroclasts erupted during individual explosions, which vary in both physical (density and crystal textures) and chemical (melt composition and volatile contents preserved in melt inclusions) characteristics, indicating evacuation of much of the conduit during each individual episode [19,20,42].

The eruption changed character after October, 1980, moving into a dominantly effusive phase. The approximately constant volume of individual dome lobes produced by these eruptions indicates that this change in style was not the result of gradual depletion of a pressurized reservoir. We suggest instead that this transition resulted from compaction and progressive closure of the transport system that slowed the ascent of individual magma quanta, permitting syn-ascent degassing and crystallization and thus reducing explosive potential. Slow ascent rates are suggested by the longer duration of the precursor LP earthquakes and deformations before each eruption episode and appear to have caused individual magma quanta to collect at a barrier below the volcano. Discrete eruptive onsets required sufficient accumulated volume prior to final magma rise to the surface. Thus it appears that the Intermediate storage system may have resumed input of approximately equal-sized magma quanta to the transport system after initial readjustment immediately following the climactic eruption of May 18, 1980, but that later eruptions were modulated by the need to achieve sufficient pressure (accumulated volume) to travel through the shallow seismic lid. The only exception to this mode of behavior came during the continuous effusion that commenced in February of 1983, which we interpret to reflect temporary development of a connected conduit between the surface and the shallow accumulation zone near the 2–3 km discontinuity. During this period, a swarm of LP earthquakes persisted during the entire extrusion episode. Activity ceased after October 1986 when the shallow lid became sufficiently strong to prevent magma passage to the surface. Ascent and intrusion in the lower transport system first became visible, in the form of VT swarms, at this time because of increasing fracture toughness of the cooling and compacting country rocks.

Alternative explanations that have been offered for both episodicity of eruptive activity and changes in eruptive style focus on variations in the dynamics of magma rise that result from rheological changes imposed by degassing and crystallization. Several models of this type were developed to explain observed variations in seismicity, rockfalls, ground tilt, and gas flux that accompanied cyclic Vulcanian explosions at Soufriere Hills volcano, Montserrat, in 1997 [e.g., [21,58–60]. Such models are consistent with observed eruptive behavior: cycles of hours to a few days culminating in Vulcanian explosions that produced clasts of variable density [61,62]. As in the summer 1980 deposits at Mount St. Helens [42], dense clasts at Montserrat represent ejection of the upper conduit plug while vesicular clasts are produced by magma from deeper in the conduit. From our perspective, this type of cyclical response is entirely consistent with the ascent of a single magma batch with near-surface modulation and we agree that it is well explained by a conduit that remains (mostly) full of magma during the time period of cyclic activity (typically weeks to a few months).

Rheologic modulation of eruptive activity has also been used, however, to explain much longer cycles of eruptive activity, cycles that include months to years of inactivity [21–23]. Important in these models is a source (either constant or variable) of magma influx into the storage system as well as feedback generated by changes in magma rheology during magma ascent toward the surface. This condition is problematic when applied to Mount St. Helens [22], however, as there is no evidence for a persistent influx of deep magma into the Mount St. Helens system. Additionally, there are several other problems with application of this type of model to the sequence of eruptive activity provided above, particularly regarding evidence for repeated development of a solidified plug within the conduit (required to explain temporary cessation of activity).

Episodic effusive eruptions at Mount St. Helens had repose intervals of 2 months (in 1981) to one year (between May 1985 and May 1986). Experimental [63–65] and observational [14,19,20,42,66] data show that time scales of weeks are sufficient for extensive crystallization and gas loss from shallow parts of the conduit. This is nicely illustrated by the current activity at Mount St. Helens, where very slow magma ascent (7–10 m/day) produces holocrystalline spines. By extrapolation, we suggest that if the conduit were completely filled with magma between effusive episodes, and if the magma were simply remobilized within the conduit because of pressure from volatile-rich magma below, the solidified plug should have been the first material pushed out of the conduit (analogous to a tube of toothpaste). However, the only extruded plugs (spines) that formed in the entire effusive sequence were (1) a spine that formed during the onset of continuous effusion in February 1983 (consistent with our interpretation that a connected shallow conduit formed at this time and therefore that shallow highly crystalline magma was extruded first) and (2) a spine that formed at the end of a protracted (17 day) extrusion event in May 1985. The latter eruption was largely endogenous [49] and the spine appears to have solidified at very shallow levels, probably within the dome itself [67]. All other dome lavas were texturally homogeneous [46,19] except for late-stage vesiculation of some dome surfaces [68]. This textural homogeneity is best explained by fairly rapid rise of individual magma batches from just beneath the seismic lid through a fracture-controlled conduit system.

To summarize, we suggest that eruptive activity at Mount St. Helens during the 1980–2006 time period presents a coherent sequence of events when viewed from the perspective of discrete magma supply, transport and eruption systems. Most important is our view of the transport system as a dynamic and changing network of cracks that varies through both time and space in magma content and connectivity and typically supplies magma to the eruptive system in small batches. In this way our view differs from traditional perspectives of stable magma conduits with simple geometries that connect the magma reservoir to the surface and vary through time only in effective diameter. Instead, we view changes in the geometry and connectedness of the transport system as fundamental in controlling the ease with which magma is transferred from the Intermediate Storage system to the Eruptive system, which in turn dictates the extent to which magma reaches the surface with its full complement of volatiles (i.e. explosively). To generalize this concept, we provide a somewhat briefer overview of another well observed modern eruption, that of Mt. Pinatubo, 1991.

3. The discrete–continuous–discrete transitions of Mt Pinatubo in 1991

3.1. Observations

As at Mount St. Helens in 1980, the awakening of Pinatubo volcano in the Philippines was signalled first by felt earthquakes on 15 March 1991 and subsequently by a phreatic explosion on April 2, 1991. Throughout April and May, small high frequency earthquakes (volcano-tectonic type, VT) accompanied several small explosions from a series of vents along the north flank of the summit dome [69], suggesting extensive fracturing. In contrast to the numerous large (M 4+) earthquakes at Mount St. Helens, however, VT earthquakes at Pinatubo had magnitudes of less than 2.5 and were clustered about 5 km NNW of the summit at depth between 3 and 7 km. Sporadic episodes of low level tremor were also observed during this period [11,70], although the intermediate depth of magma intrusion limited degassing and resulting LP earthquakes during the first weeks of activity. This picture changed on May 26 with the appearance of deep LP earthquakes soon followed by shallow LP events [11,70,71]. This change in the seismicity was followed by a tenfold increase in SO_2 emissions (500 to 5000 tons/day), far greater than any pre-eruptive gas emissions from Mount St. Helens [69]. Pallister et al. [72] and White et al. [71] suggest that the deep LP earthquakes marked the intrusion of basaltic magma into the intermediate storage system.

A new swarm of deep LP events occurred on the 28th of May. A drastic reduction in SO_2 emissions to 1400 tons/day on May 30 [69] was followed by earthquake migration to 1 km northwest of the summit at a depth of ≤5 km. By June 3, shallow magma intrusion had produced small ash explosions, episodes of harmonic tremor, and distinct inflation measured by an electronic tiltmeter close to the summit. Seismicity continued to increase until an explosion on June 7 generated a 6–7 km high column of steam and ash. This activity culminated in a series of explosions on June 7–8. The next day, a small lava-dome emerged close to the fuming vents.

From June 8 to June 12, weak ash emissions, episodes of harmonic tremor, swarms of VT earthquakes, and shallow LP events provided evidence of both brittle fracture and degassing. A burst of intense harmonic tremor (40 min long) at 03:01 on June 12 signaled a new explosive event, a precursor to the first major ash eruption at 08:51 [70]. This eruption was followed by an unusual seismic signal, called the "Groan" [70], that consisted of a continuous string of VT earthquakes with the peak energy shifting three times to a lower frequency band for short periods. It was interpreted [70] as movement of magma and associated volatiles in a new system of cracks and passageways.

Three more vertical explosive eruptions occurred with decreasing intensity from June 12 through June 14, with 2- to 4-hour precursory LP swarms suggesting increasing ascent velocities during this time period. The last vertical eruption occurred on June 14 at 13:09. Throughout the rest of June 14 and morning of June 15, thirteen large surge-producing explosions occurred at decreasing time intervals. The later eruptive pulses evolved into a continuous strong, seismic signal that saturated the instruments by 13:42, signaling the onset of the climactic eruption. Although the size of individual eruptive events during this time period is not known, the total ash volume produced by the three vertical and thirteen surge events was approximately 10^8 m^3 DRE [73], yielding an average volume for each event of 6×10^6 m^3, similar to the volume of ash produced by the initial vertical eruption on June 12. This time period also marked a gradual change in the composition of the erupted material from andesite to dacite [72,74].

The increasing frequency of pulsating activity prior to the beginning of the climactic eruption on June 15 points to an increasing supply of magma. Evidence for increasing rates of magma ascent is provided by textural changes in the eruptive products [14,75], in particular, in the wide range in density (vesicularity) and crystallinity of clasts from individual surge events (Fig. 5A). Constant measured H_2O contents of 1–2 wt.% in the matrix glass of dense juvenile clasts indicate temporary magma residence (equilibration) at pressures of 7.5–27.5 MPa. However, the corresponding crystallinity of these samples is much lower than experimentally determined equilibrium values for these pressures (Fig. 5B) [14], an indication of the kinetic lag time between degassing and crystallization and the short residence time of the magma at shallow pressures. Hoblitt et al. [73] recognized that this pulsatory precursory activity required episodic delivery of individual magma batches to the vent at increasing rates and with decreasing impedance through time.

The eruption′s most violent explosive phase began at 13:42 on June 15 and continued for more than 15 h at full strength, generating an eruption column with a height of 30–40 km and pyroclastic flows that spread over distances of 12–18 km from the vent [69]. Strong earthquakes (magnitudes 4.8 to 5.6) felt throughout the night of June 15 were probably associated with the collapse of the Intermediate Storage system to form a nearly circular caldera of about 2 km in diameter.

After the climactic event, tephra emission continued at decreasing rates over the subsequent 3 months; this decline was punctuated from late June throughout most of July by moderate explosions accompanied by episodes of harmonic tremor. The eruptions ejected

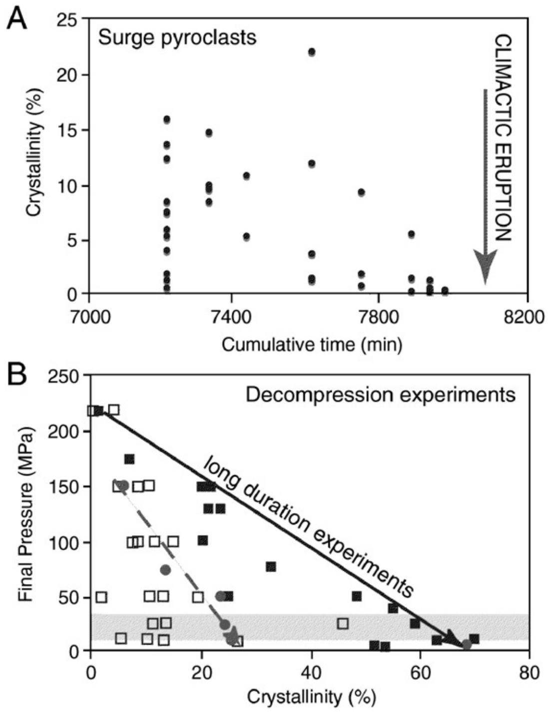

Fig. 5. Decompression-induced crystallization of Pinatubo magma. (A) Variations in the crystallinity of dense juvenile clasts from surge deposits 3 through 10, shown as a function of cumulative time since the first appearance of the lava dome on June 8. Note the general trend of decreasing crystallinity with time (data from [14]). (B) Experimentally determined crystallinity of Pinatubo magma originally H_2O-saturated at 220 MPa and 780 °C and decompressed at different rates (data from [63]). Solid arrow drawn through solid squares shows the equilibrium decompression–crystallization trend for experiments of long duration (160–931 h). Dashed arrow drawn through solid circles shows the decompression trend for multi-step decompression experiments performed to simulate steady magma decompression at a rate of 1.2 MPa/h (equivalent to approximately 0.01 m/s). Gray bar shows equilibration pressures recorded by H_2O content of the matrix glass in the surge samples.

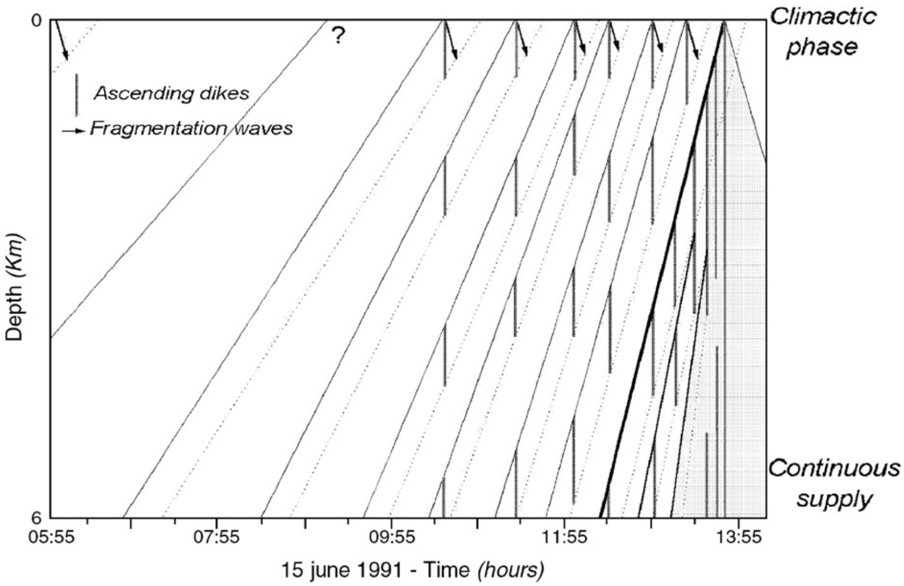

Fig. 6. Sketch of the ascent of the surge producing eruptions of Pinatubo leading to the climactic phase on June 15, 1991. The sequence is characterized by increasing ascent velocities (steeper slope) and higher supply. Individual explosive eruptions are generated by downward propagation of a fragmentation wave (arrows) through individual magma batches (continuous line) as they reach the surface. The climactic phase of the eruption occurs when individual magma quanta coalesce to allow a continuous magma supply to the surface.

ash clouds that at times reached to 15–16 km height [74]. Continuous ash emission ceased by August 1, 1991. The last small explosive eruption occurred on September 4. As at Mount St. Helens, lava effusion then followed in the summer of 1992 from mid-July through October [69]. This effusive phase of the eruption was preceded by seismic swarms and tremor beginning on July 3. Seismic activity again increased on February 8–11, 1994 and on January 7, 1995, with episodes of harmonic tremor, explosion-related earthquakes and VT events. This seismicity closely resembles the post 1986 activity of Mount St. Helens, when a series of intrusions at depth were unable to reach the surface. The much more rapid diminution of eruptive activity at Mt. Pinatubo relative to that at Mount St. Helens may reflect the much more extensive draining of the magma reservoir during the climactic caldera-forming phase of the Pinatubo eruption.

3.2. Interpretation

We believe that the Mt. Pinatubo eruption sequence is also illuminated by consideration of the role of magma quanta in the development, and eventual closure, of the transport system. In particular, we examine the spatio-temporal variations in precursory seismicity, the protracted onset of eruptive activity, and the post-climactic eruption sequence.

Of particular importance at Pinatubo is the relationship between the seismic precursors and patterns of gas emission. We agree that the correlation between the appearance of deep LPs and ten-fold increase in SO_2 emissions in late May reflects the input of basaltic magma into the storage region. We extend this to suggest that the abrupt increase in SO_2 emissions indicates that a fracture network within the transport system had already formed prior to the deep intrusion. This is consistent with the deep swarm following, by almost two months, the onset of shallow unrest. SO_2 emissions then decreased suddenly on May 30. We suggest that this decrease, together with the migration of earthquake locations, records the first intrusion of magma into the fracture network (lower transport system). At this point, magma intrusion inhibited continued degassing of the Intermediate Storage System. Ascent of early magma from the Intermediate Storage system to the surface between May 30 and June 7 culminated in the eruptions of June 7–8. An estimated average magma ascent rate for this time period of 0.01 m/s is comparable to that inferred for early batches rising beneath Mount St. Helens in March 1980 as well as those estimated for domes that accompanied early explosive activity. Slow ascent is also consistent with the highly crystallized groundmass of the dome lava [14,72].

The swarms of VT earthquakes and shallow LP events that dominated the seismic record between June

8 and 12 provide evidence of brittle fracture and degassing that we interpret as fracturing and intrusion of magma into the Transport System. Explosive activity on June 12 provides more specific constraints on magma ascent, with transport of a single magma batch (4–6×10^6 m^3 DRE) from the Intermediate Storage system at 8 km depth to the surface apparently occurring between 03:01 and 08:51, yielding an average ascent velocity of 0.38 m/s. This rate is comparable with the velocity of magma batches rising at Mount St. Helens during the summer of 1980 and suggests increasing ease of magma ascent through the increasingly fractured Transport System. The variable compositions and microphenocryst contents of the erupted products [14,73] show that this magma quantum sampled batches of magma residing at different depths.

The June 12 eruption was followed by the unusual seismic "Groan", a signal that we interpret to record the opening of a semi-continuous pathway that facilitated ascent of subsequent magma quanta. Over the next few days, the decreasing time between eruptive pulses indicates that a large part of the Transport System was occupied by ascending quanta. This sequence of events can also be viewed as a gradual increase in connectivity of the Transport system, which permitted increasingly easy access of the magma to the surface. The last surge events completed the connectivity of the transport system, setting the stage for the climactic eruption (Fig. 6). Importantly, we view the culmination of the eruption in caldera collapse to be the logical consequence of a completely connected transport system, which also permitted extraordinarily high rates of magma discharge (4×10^8 kg/s) and ascent velocities (>5–10 m/s) as the fragmentation wave reached the Intermediate Storage System [75].

As at Mount St. Helens, activity following the climactic eruption records the gradual closing of the transport system. The high tephra and gas emissions that persisted throughout the summer of 1991 reflect an open fracture network. Depletion of magma from the storage region during the climactic eruption, however, provided insufficient magma to feed further steady eruptions. With time, the transport system closed enough to allow sufficient pressurization for renewed ascent of small magma batches to produce a dome. During the effusive phase, individual magma batches ascended with progressively slower velocities (<0.01 m/s), reflecting the increased difficulty of magma movement through the conduit.

4. Discussion and conclusions

Our interpretive model provides a simple framework that not only explains the observed sequence of eruptive phenomena at both Mount St. Helens and Pinatubo but

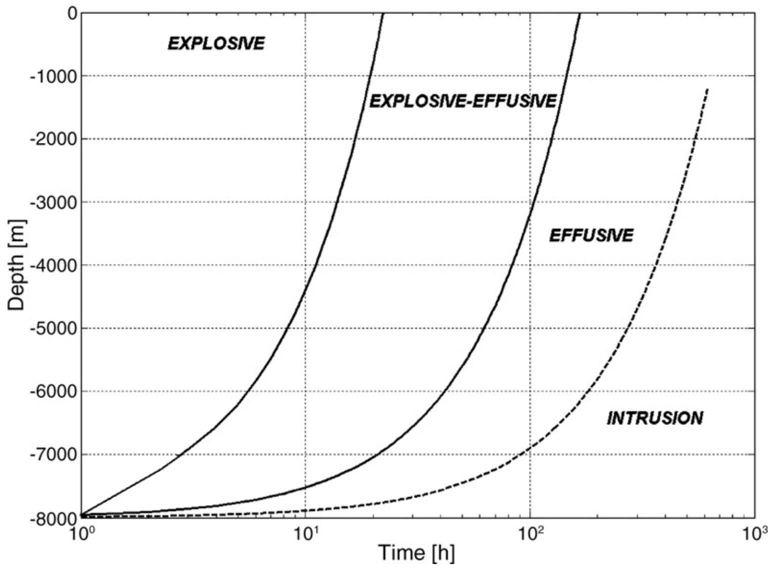

Fig. 7. Eruptive style is controlled by the time of magma ascent from a mid-crustal magma chamber. The continuous line defining the Explosive field is evaluated by the ascent velocities for the explosive eruptions of St. Helens and Pinatubo and implies velocities higher than that shown in the graph. The continuous line defining the Effusive field is based on ascent velocities of the earlier cryptodome event at Mount St. Helens and the dome eruptions at Pinatubo and implies velocity lower than that shown in the graph. In between the two continuous lines is a field where both types of activity are likely, as in the summer 1980 eruptions of St. Helens. The dashed line suggests a lower velocity limit for the intrusion events with ascent times longer than months.

also provides insight into the significance of different eruptive precursors. Although the model is based on observational evidence gathered during the eruption of Mount St. Helens, its success in explaining the temporal evolution of the 1991 Pinatubo eruption suggests that it may have widespread application for understanding the onset of eruptive activity. Of primary importance is the interplay among the Supply System, Intermediate Storage System, and Transport System, which may not be as straightforward as generally thought. In particular, the development of the Transport System is a complex process that follows a different course from eruption to eruption, thus explaining the variety of behaviors displayed by awakening volcanoes.

An important observation related to the development of the Transport System is that a shallow fracture network can develop prior to, rather than directly associated with, magma intrusion. This is illustrated by precursory VT seismicity that commonly lacks other evidence of magma migration such as Long Period earthquakes, tremor events, elevated SO_2 emissions, or local uplift. Pinatubo provides one example of this behavior. Another example is Spurr volcano, Alaska, where VT earthquakes recorded a 90° stress field rotation several months before the eruption of Crater Peak in 1992 [76]. The long time lag between the beginning of this change and the eruption, as well as the lack of other precursory signals, suggests magma intrusion may not have been directly responsible for early precursors. This interpretation is supported by (1) changes in the crater lake color shortly before the eruption, signaling the arrival of magmatic gases to the near-surface environment and (2) studies of the eruptive products that indicate rapid rise of individual magma batches from the magma storage region to the surface during each of the three eruptive events [13]. Importantly, such temporal (and spatial) separation of fracture patterns from magma intrusion indicates that seismic swarms and volatile emissions may not always presage eruptive activity. At Pinatubo, the opening of a fracture network in the Transport system was apparently necessary but not sufficient to start magmatic activity. The incorporation of hot basaltic magma batches into the Intermediate Storage System at Pinatubo may have stimulated the increasing supply and ascent rate of magma quanta that ultimately created the bottom-up connectivity of the Transport System.

We summarize the observations presented above by defining different styles of activity based on limiting ascent velocities of silicic magmas fed by mid-crustal magma chambers (Fig. 7). Velocities are calculated for explosive events using the time between the observation of tremor events and the beginning of the explosive episode and assuming a reservoir depth of 8 km [38,72] for consistency with the velocity of magma ascent estimated for the climax of the May 18 eruption. The ascent velocity leading to dome growth is estimated using the duration of the precursory LP events. As LPs occur at depths $\ll$ 8 km, estimated velocities are minima. Episodes of mixed explosive–effusive activity that occurred at Mount St. Helens on June 12 and August 7, 1980, have multiple precursor signals, suggesting the possible interaction of magma quanta having different velocities.

The graph of Fig. 7 shows that the time spent in the transport system, and especially at shallow depth, entirely controls degassing, and thus eruptive style (explosive vs. effusive). While this concept is not new [21,34], our perspective – that the episodic ascent of single magma batches detached from the Intermediate Storage system is key to understanding the development of Transport Systems – presents an alternative view to that of long-lived, fully connected volcanic conduits. We consider batch-like, rather than steady, magma supply to be the normal mode in silicic systems.

Another key aspect of our conceptual model is the observation that climactic eruptions occur only with the development of a fully connected conduit. Connectivity may develop either downward, by decompression and fragmentation of multiple ascending magma batches, or upward, by increasing rates of magma supply from below, or some combination of the two. Of our two examples, connectivity along the conduit at Mount St. Helens apparently developed primarily by downward propagation of a decompression wave triggered by the collapse of the volcano′s north flank, while connectivity along the Pinatubo conduits seems to have developed by increasing amounts of magma supplied from below. One important consequence of the gradual construction of a connected conduit over time periods of days to weeks may be a gradual decrease in the effective pressure of the Intermediate Storage system from lithostatic to ‘magmastatic’. This pressure decrease may be reflected in late-stage decompression-driven crystallization that provides the appearance of pre-eruptive magma ascent to intermediate levels [77,78]. For example, in their experimental study of Pinatubo magma, Hammer and Rutherford [78] note a mismatch between magma storage pressures recorded by hornblende compositions (220 MPa) and those of the matrix glass (144–164 MPa). A reduction in effective pressure of 70 MPa could be achieved either by fluxing with CO_2 [78], upward migration of magma of almost 3 km [74], or by a 30% reduction in the average density of the overburden. It seems likely that some combination of these processes was at work during the days immediately preceding the climactic event. Interestingly, the same pressure decrease is required to explain differences between the inferred storage region at 220 MPa and glass compositions suggesting equilibration at water pressures as low as 150 MPa for magma erupted from Mount St. Helens on May 18 [20,77]. This implies some amount of bottom-up magma migration preceding the climactic eruption at Mount St. Helens, as well, perhaps related to episodic magma supply to the growing cryptodome.

In summary, we suggest that a view of magma conduits as transient and dynamic provides an important perspective from which both geophysical and geochemical data can be re-interpreted to relate changing conditions of magma storage and migration to observed eruptive phenomena. We believe that existing models of connected conduits can fully explain large scale explosive eruptions, but that they are not fit to describe smaller events, particularly where the volume of erupted magma does not fill an entire conduit. Within the outlined framework, it is easier to understand the occurrence of large scale eruptions that occur only under particular conditions related with the mechanism of ascent. Finally, we believe that this model may yield important new insights into the nature of eruptive precursors, thereby improving our predictive capabilities, and stimulate a fruitful discussion on the mechanism of ascent of magmas.

Acknowledgements

Two anonymous referees greatly improved the original manuscript; in particular one of them, who did not share our views, pointed out critical weaknesses of the original presentation. We acknowledge Lisetta Giacomelli for years-long discussions and sound geological suggestions, Elisabetta Mattei for allowing reproduction of Fig. 6 from her unpublished thesis, and Francesca Fattori-Speranza for drawing of Figs. 2 and 7. We thank Linda Malone for her dining room table and enthusiastic support of our ideas.

RS acknowledges partial financial support from INGV and Dipartimento Protezione Civile Nazionale of Italy, and MIUR-Prin Project 2005 (Risalita dei Magmi e Dinamica delle Eruzioni). KVC acknowledges support of National Science Foundation grants EAR0207362 and EAR0510437.

References

[1] S.D. Malone, C. Boyko, C.S. Weaver, Seismic precursors to the Mt St Helens eruptions in 1981 and 1982, Science 221 (1983) 1376–1378.

[2] D.A. Swanson, T.J. Casadewall, D. Dzurisin, S.D. Malone, C. Newhall, C.S. Weaver, Predicting eruptions at Mt St Helens, Science 221 (1983) 1369–1376.

[3] W. Marzocchi, L. Sandri, P. Gasparini, C. Newhall, E. Boschi, Quantifying probabilities of volcanic events: the example of volcanic hazard at Mount Vesuvius, J. Geophys. Res. 109 (2004), doi:10.1029/2004JB003155.

[4] M. Feuillard, C.J. Allegre, G. Brandeis, R. Gaulon, J.L. Le Mouel, J.C. Mercier, J.P. Pozzi, M.P. Semet, The 1975–1977 crisis of La Souftriere De Guadalupe (FWI): a still born magmatic eruption, J. Volcanol. Geotherm. Res. 16 (1983) 317–334.

[5] S.M. Bower, A.W. Wood, On the influence of magma chambers in controlling the evolution of explosive volcanic eruptions, J. Volcanol. Geotherm. Res. 86 (1998) 67–78.

[6] S. Blake, Volcanism and the dynamics of open magma chamber, Nature 289 (1981) 783–785.

[7] C.R.J. Kilburn, Multiscale fracturing as a key to forecasting volcanic eruptions, J. Volcanol. Geotherm. Res. 125 (2003) 271–289.

[8] C.R.J. Kilburn, P.R. Sammonds, Maximum warning times for imminent volcanic eruptions, Geophys. Res. Lett. 32 (2005), doi:10.1029/2005GL024184.

[9] D.C. Roman, K.V. Cashman, The origin of volcano-tectonic earthquake swarms, Geology 34-6 (2006) 457–460.

[10] E. Endo, S.D. Malone, L.S. Noson, C.S. Weaver, Locations, magnitudes and statistics of the March 20–May 18 earthquake sequence, U. S. Geol. Surv. Prof. Pap. 1250 (1981) 93–108.

[11] D.H. Harlow, J.A. Power, E. Laguerta, G. Ambubuyong, R.A. White, R.P. Hoblitt, Precursory seismicity and forecasting of the June 15, 1991, eruption of Mount Pinatubo, in: C.G. Newhall, R.S. Punongbayan (Eds.), Fire and Mud, Univ. of Wash. Press, Seattle, 1996, pp. 285–306.

[12] M. Bursik, Subplinian eruption mechanisms inferred from volatile and clast dispersal data, J. Volcanol. Geotherm. Res. 57 (1993) 57–70.

[13] C.A. Gardner, K.V. Cashman, K.A. Neall, Tephra-fall deposits from the 1992 eruption of Crater Peak, Alaska: implications of clast textures for eruptive processes, Bull. Volcanol. 59 (1998) 537–555.

[14] J.E. Hammer, K.V. Cashman, R.P. Hoblitt, S. Newman, Degassing and microlite crystallization during the pre-climactic events of the 1991 eruption of the Mt. Pinatubo, Philippines, Bull. Volcanol. 60 (1999) 355–380.

[15] L. Wilson, R.S.J. Sparks, G.P.L. Walker, Geophys. Explosive volcanic eruptions — IV. The control of magma properties and conduit geometry on eruption column behaviour, Geophys. J. R. Astron. Soc. 63 (1980) 117–148.

[16] L. Wilson, J.W. Head, Ascent and emplacement of basaltic magmas on the Earth and Moon, J. Geophys. Res. 86 (1981) 2971–3001.

[17] J.C. Eichelberger, C.R. Carrigan, H.R. Westrich, R.H. Price, Non explosive silicic volcanism, Nature 323 (1986) 598–605.

[18] C. Jaupart, C.J. Allegre, Gas content, eruption rate and instabilities of eruption regime in silicic volcanoes, Earth Planet. Sci. Lett. 102 (1991) 413–429.

[19] K. Cashman, J. Blundy, Degassing and crystallization of ascending andesite and dacite, Philos. Trans. R. Soc. Lond. Ser. A 358 (2000) 1487–1513.

[20] J. Blundy, K. Cashman, Rapid decompression-driven crystallisation recorded by melt inclusions from Mount St. Helens volcano, Geology 33 (2005) 793–796.

[21] O. Melnik, R.S.J. Sparks, Dynamics of Magma Ascent and Lava Extrusion at Soufriere Hills Volcano, Montserrat, Mem. Geol. Soc. Lond. 21 (2002) 153.

[22] A. Barmin, O. Melnik, R.S.J. Sparks, Periodic behaviour in lava dome eruptions, Earth Planet. Sci. Lett. 199 (2002) 173–184.

[23] O. Melnik, R.S.J. Sparks, Controls on conduit magma flow dynamics during lava dome building eruptions, J. Geophys. Res. 110 (2005), doi:10.1029/2004JB003183.

[24] P.D. Bons, J. Dougherty-Page, M.A. Elburgh, Stepwise accumulation and ascent of magmas, J. Metamorph. Geol. 19 (2001) 625–631.

[25] P.D. Bons, J. Arnold, M.A. Elburg, J. Kalda, A. Soesoo, B.P. van Milligen, Melt extraction and accumulation from partially molten rocks, Lithos 78 (2004) 25–42.

[26] R.S.J. Sparks, S.R. Young, The eruption of Soufrière Hills volcano, Montserrat (1995–1999): overview of scientific results, in: T.H. Druitt, B.P. Kokelaar (Eds.), The Eruption of the Soufrière Hills Volcano, Montserrat From 1995 to 1999, Mem. Geol. Soc. London, vol. 21, 2002, pp. 45–69.

[27] M.P. Ryan, Neutral buoyancy and the mechanical evolution of magmatic system, The Geochemical Soc. Special Publication, vol. 1, 1987, pp. 259–287.

[28] S.R. McNutt, Volcanic seismicity, in: H. Sigurdsson (Ed.), Encyclopedia of Volcanoes, Academic Press, San Diego, 2000, pp. 1015–1033.

[29] T. Menard, S. Tait, The propagation of a buoyant liquid-filled fissure from a source under constant pressure: an experimental approach, J. Geophys. Res. (2002), doi:10.1029/2001JB000589.

[30] J. Weertman, Theory of water-filled crevasses in glaciers applied to magma transport beneath oceanic ridges, J. Geophys. Res. 76 (1971) 1171–1183.

[31] D.D. Pollard, O.H. Muller, The effects of gradients in regional stress and magma pressure on the form of sheet intrusions in cross section, J. Geophys. Res. 81 (1976) 975–984.

[32] M. Mangan, T. Sisson, Delayed, disequilibrium degassing in rhyolite magma: decompression experiments and implications for explosive volcanism, Earth Planet. Sci. Lett. 183 (2000) 441–455.

[33] C. Klug, K.V. Cashman, Vesiculation of May 18, 1980, Mt St Helens magma, Geology 22 (1994) 468–472.

[34] K.V. Cashman, Volatile controls on magma ascent and eruption, The State of the Planet: Frontiers and Challenges in Geophysics", American Geophysical Union Monograph, vol. 150, 2004, pp. 109–124.

[35] P.W. Lipman, D.R. Mullineaux (Eds.), The 1980 Eruption of Mt St Helens, Washington, U. S. Geol. Surv. Prof. Pap., vol. 1250, 1981, p. 1.

[36] K.V. Cashman, R.P. Hoblitt, Magmatic precursors to the 18 May 1980 eruption of Mount St. Helens, USA, Geology 32 (2004) 141–144.

[37] P.W. Lipman, J.G. Moore, D.A. Swanson, Bulging of the north flank before the May 18 eruption. Geodetic data, U. S. Geol. Surv. Prof. Pap. 1250 (1981) 143.

[38] R. Scandone, S.D. Malone, Magma supply, magma discharge and readjustment of the feeding system of Mount St. Helens during 1980, J. Volcanol. Geotherm. Res. 23 (1985) 239–252.

[39] C.W. Criswell, Chronology and pyroclastic stratigraphy of the May 18,1980 eruption of Mount St. Helens, Washington, J. Geophys. Res. 92 (1987) 10237–10266.

[40] P.D. Rowley, M.A. Kuntz, N.S. MacLeod, Pyroclastic flow deposits, U. S. Geol. Surv. Prof. Pap. 1250 (1981) 489–512.

[41] J. Blundy, K. Cashman, K. Berlo, A volcano rekindled: the first year of renewed eruption at Mount St. Helens, 2004–2006, in: D.R. Sherrod, W. Scott (Eds.), U.S. Geological Survey Prof. Paper (in press).

[42] K.V. Cashman, S.M. McConnell, Multiple levels of magma storage during the 1980 summer eruptions of Mount St. Helens, WA, Bull. Volcanol. (2005), doi:10.1007/s00445-005-0422.

[43] T.J. Casadevall, D.A. Johnston, W.I. Rose, L.L. Malinconico, R.E. Stoiber, T.J. Borhnost, S.N. Williams, SO_2 emission rates at Mt St Helens from March 29 trough December 1980, in: P.W. Lipman, D.R. Mullineaux (Eds.), U.S. Geological Survey Prof. Pap., vol. 1250, 1981, pp. 193–200.

[44] D.A. Swanson, P.W. Lipman, J.G. Moore, C.C. Heliker, K.M. Yamashita, Geodetic monitoring after the May 18, eruption, in: P.W. Lipman, D.R. Mullineaux (Eds.), U.S. Geological Survey Prof. Pap., vol. 1250, 1981, pp. 157–168.

[45] G. Neri, S.D. Malone, An analysis of the earthquake time series at Mt St Helens, Washington in the framework of recent volcanic activity, J. Volcanol. Geotherm. Res. 38 (1989) 257–267.

[46] K.V. Cashman, Groundmass crystallization of Mount St. Helens dacite, 1980–1986: a tool for interpreting shallow magmatic processes, Contrib. Mineral. Petrol. 109 (1992) 431–442.

[47] C. Geschwind, M.J. Rutherford, Crystallization of microlites during magma ascent: the fluid mechanics of 1980–1986 eruptions at Mount St. Helens, Bull. Volcanol. 57 (1995) 356–370.

[48] D.A. Swanson, R.T. Holcomb, Regularities in growth of the Mt St Helens Dacite Dome, 1980–1986, in: J.H. Fink (Ed.), Lava Flows and Domes. Emplacement Mechanisms and Hazard Implications, Springer, New York, 1991, pp. 3–24.

[49] J.H. Fink, M.C. Malin, S.W. Anderson, Intrusive and extrusive growth of the Mount St. Helens lava dome, Nature 348 (1990) 435–437.

[50] M.J. Fremont, S.D. Malone, High precision relative locations of earthquakes at Mount St. Helens, Washington, J. Geophys. Res. 92 (1987) 10223–10236.

[51] S.C. Moran, Seismicity at Mount St. Helens, 1987–1992: evidence for repressurization of an active magmatic system, J. Geophys. Res. 99 (1994) 4341–4354.

[52] C. Musumeci, S. Gresta, S.D. Malone, Magma system recharge of Mount St. Helens from precise relative hypocenter location of microearthquakes, J. Geophys. Res. 107 (2002), doi:10.1029/2001JB000629.

[53] E.Y. Iwatsubo, L. Topinka, D.A. Swanson, Slope distance measurements to the flanks of Mount St Helens, late 1980 through 1989, USGS Bull. 1966 (1992) 85–94.

[54] D.M. Harris, W.I. Rose, R. Roe, M.R. Thompson, Radar observations of ash eruptions, U. S. Geol. Surv. Prof. Pap. 1250 (1981) 335–346.

[55] S. Carey, H. Sigurdsson, The May 18, 1980 eruption of Mt St Helens. 2 Modeling of dynamics of the plinian phase, J. Geophys. Res. 90 (1985) 2948–2958.

[56] J.E. Shemeta, C.S. Weaver, Seismicity accompanying the May 18,1980 eruption of Mount St. Helens, Washington, in: S.A.C. Keller (Ed.), Mt St. Helens: Five Years Later, Eastern Washington University Press, Cheney, WA, 1986, pp. 44–58.

[57] K. Berlo, J. Blundy, S. Turner, K.V. Cashman, C. Hawkesworth, S. Black, Geochemical precursors to volcanic activity? Timescales of degassing at Mount St. Helens, USA, Science 306 (2004) 1167–1169.

[58] R.P. Denlinger, R.P. Hoblitt, Cyclic eruptive behavior of silicic volcanoes, Geology 27 (1999) 459–462.

[59] B. Voight, R.S.J. Sparks, A.D. Miller, A. Clarke, J. Ewart, W.P. Aspinall, B. Baptie, E.S. Calder, P. Cole, T.H. Druitt, C. Hartford, R.A. Herd, P. Jackson, A.M. Lejeune, A.B. Lockhart, S.C. Loughlin, R. Luckett, L. Lynch, G.E. Norton, R. Robertson, I.M. Watson, R. Watts, S.R. Young, Magma flow instability and cyclic

activity at Soufriere Hills Volcano, Montserrat, British West Indies, Science 283 (1999) 1138–1142.
[60] J.J. Wylie, B. Voight, J.A. Whitehead, Instability of magma flow from volatile-dependent viscosity, Science 285 (1999) 1883–1885.
[61] Y. Formenti, T.H. Druitt, Vesicle connectivity in pyroclasts and implications for the fluidisation of fountain-collapse pyroclastic flows, Montserrat (West Indies), Earth Planet. Sci. Lett. 214 (2004) 561–574.
[62] Y. Formenti, T.H. Druitt, K. Kelfoun, Characterisation of the 1997 Vulcanian explosions of Soufrière Hills Volcano, Montserrat, by video analysis, Bull. Volcanol. (2004), doi:10.1007/s00445-003-0288-8.
[63] J.E. Hammer, M. Rutherford, An experimental study of the kinetics of decompression-induced crystallization in silicic melt, J. Geophys. Res 107 (2002) (doi: 10.1029).
[64] S. Couch, R.S.J. Sparks, M.R. Carroll, The kinetics of degassing-induced crystallization at Soufriere Hills Volcano, Montserrat, J. Petrol. 44 (2003) 1477–1502.
[65] C. Martel, B.C. Schmidt, Decompression experiments as an insight into ascent rates of silicic magmas, Contrib. Mineral. Petrol. 144 (2003) 397–415.
[66] H. Wright, K.V. Cashman, M. Rosi, R. Cioni, Breadcrust bombs as indicators of eruption dynamics at Pichincha volcano, Ecuador, Bull. Volcanol. (2006), doi:10.1007/s00445-006-0073-6.
[67] K.V. Cashman, C.R. Thornber, J.S. Pallister, From dome to dust: shallow crystallization and fragmentation of conduit magma during the 2004–2006 dome extrusion of Mount St. Helens, in: D.R. Sherrod, W. Scott (Eds.), U.S. Geological Survey Prof. Paper (in press).
[68] S.W. Anderson, J.H. Fink, W.I. Rose, Mount St. Helens and Santiaguito lava domes: the effect of short-term eruption rate on surface texture and degassing processes, J. Volcanol. Geotherm. Res. 69 (1995) 105–116.
[69] E.W. Wolfe, R.P. Hoblitt, in: C.G. Newhall, R.S. Punongbayan (Eds.), Overview of the Eruptions in “Fire and Mud”, Univ. of Wash. Press, Seattle, 1996, pp. 3–20.
[70] J.A. Power, T.L. Murray, J.F. Marso, E.P. Laguerta, Preliminary observation of seismicity by use of the Seismic Spectral Amplitude Measurement (SSAM) system May 13, June 18, in: C.G. Newhall, R.S. Punongbayan (Eds.), Fire and Mud, Univ. of Wash. Press, Seattle, 1996, pp. 269–284.
[71] R.A. White, Precursory deep long period earthquakes at Mt Pinatubo, in: C.G. Newhall, R.S. Punongbayan (Eds.), Fire and Mud, Univ. of Wash. Press, Seattle, 1996, pp. 307–328.
[72] J.S. Pallister, R.P. Hoblitt, G.P. Meeker, R.J. Knight, D.F. Siems, Magma mixing at Mt Pinatubo: petrographic and chemical evidence from the 1991 deposits, in: C.G. Newhall, R.S. Punongbayan (Eds.), Fire and Mud, Univ. of Wash. Press, Seattle, 1996, pp. 687–732.
[73] R.P. Hoblitt, E.W. Wolfe, W.E. Scott, M.R. Couchman, J.S. Pallister, D. Javier, The preclimactic eruptions of Mount Pinatubo, June 1991, in: C.G. Newhall, R.S. Punongbayan (Eds.), Fire and Mud, Univ. of Wash. Press, Seattle, 1996, pp. 457–512.
[74] M.L. Paladio-Melosantos, R.U. Solidum, W.E. Scott, R.B. Quiambao, J.V. Umbal, K.S. Rodolfo, B.S. Tubianosa, P.J. Delos, R.A. Reyes Alonso, H.B. Ruelo, Tephra falls of the 1991 eruptions of Mount Pinatubo, in: C.G. Newhall, S. Punongbayan (Eds.), Fire and Mud, Univ. of Wash. Press, Seattle, 1996, pp. 513–535.
[75] M. Polacci, P. Papale, M. Rosi, Textural heterogeneities in pumices from the climactic eruption of Mount Pinatubo, 15 June 1991, and implications for magma ascent dynamics, Bull. Volcanol. 63 (2001) 83–96.
[76] D.C. Roman, S.C. Moran, J.A. Power, K.V. Cashman, Temporal and spatial variation of local stress fields during the 1992 eruptions of Crater Peak (Mt. Spurr), Alaska, Bull. Seismol. Soc. Am. 94 (2004) 2366–2379.
[77] J. Blundy, K.V. Cashman, Ascent-driven crystallisation of dacite magmas at Mount St. Helens, 1980–1986, Contrib. Mineral. Petrol. 140 (2001) 631–651.
[78] J.E. Hammer, M. Rutherford, Petrologic indicators of preeruption magma dynamics, Geology 31 (2003) 79–82.